

Novel 1.5' Size Exceptional PMTs for the CTA Project

Razmik Mirzoyan^{1,2}, Dominik Müller², Takeshi Toyama², Daisuke Nakajima³, Uta Menzel², Jürgen Hose², Mitsunari Takahashi³, Tokonatsu Yamamoto⁴, Masahiro Teshima^{2,3}

²Max-Planck-Institute for Physics, Munich, Germany; ³ICRR, University of Tokyo, Chiba, Japan;

⁴Konan University, Japan

E-mail: Razmik.Mirzoyan@mpp.mpg.de

Abstract. Photo Multiplier Tubes (PMT) are the most wide-spread detectors for measuring fast, faint light signals. About seven years ago we started an improvement program for the PMT candidates for the Cherenkov Telescope Array (CTA) project with the companies Hamamatsu Photonics K.K. (Japan) and Electron Tubes Enterprises Ltd. (England). CTA is the next major Imaging Atmospheric Cherenkov Telescopes array for high energy gamma-ray astrophysics; about 100 telescopes of sizes of 23m, 12m and 4m in diameter will be built in the Northern and Southern hemispheres. For CTA we need PMTs with the highest possible quantum efficiency, maximized photo electron collection efficiency, short pulse width of a few ns, very low after-pulsing and transit time spread. After several iterations the manufacturers were able to produce 1.5' PMTs of enhanced peak quantum efficiency of $\sim 40\%$. These can collect up to 95-98% of photo electrons onto the first dynode for the wavelengths $\geq 400\text{nm}$. A pulse width of $\leq 3\text{ns}$ has been achieved at the selected operational gain of 40k. The after-pulsing for a threshold of ≥ 4 photo electrons is reduced to the level of 0.02%. We report on the measurements of PMT R-12992-100 from Hamamatsu, which is already a commercial product and the PMT D573KFLSB from Electron Tubes Enterprises. The latter is not the final PMT but the latest iteration towards the candidate sensor for the CTA project.

International Conference on New Photo-detectors

PhotoDet2015

6-9 July 2015

Moscow, Troitsk, Russia

¹Speaker

1. Introduction

Currently the standard light sensors for the Imaging Atmospheric Cherenkov Telescopes (IACT) are the classical Photo Multiplier Tubes (PMT) of bialkali type photo cathode. A major component of IACTs is the imaging camera in the focus of a large reflector. About seven years ago we started a dedicated development program with the PMT manufacturers Hamamatsu Photonics K.K. (Japan) and Electron Tubes Enterprises Ltd. (ETE, England) for novel PMTs for the Cherenkov Telescope Array (CTA) project. We defined a wish-list of key parameters of the needed 1.5' size PMTs and requested both companies to work on improving those.

CTA is the next generation IACT observatory for very high energy gamma ray astrophysics [1]. CTA will cover the energy range from a few tens of GeV to above 100 TeV. The goal of this project is to perform diverse astrophysical studies with a sensitivity that is about one order of magnitude higher than what is currently available in operating major IACTs VERITAS, H.E.S.S. and MAGIC [2-4].

As a result of this campaign, PMTs of outstanding good parameters became available, about which we will report below.

2. Classical PMTs with bialkali photo cathode for CTA

After multiple iterations over a time span of several years, by merging the best design features of Hamamatsu R9420 (1.5') and Hamamatsu R 8619 (1') PMTs, and by introducing a good number of improvements, Hamamatsu produced the 8-dynode PMT R11920-100 [5]. Though the main parameters of this PMT showed to be outstanding, still the requested pulse width of 3.0ns at the operational gain of 40k could not be achieved. Instead, it showed a pulse width of $\sim(3.7-3.9)$ ns. For overcoming this problem Hamamatsu reduced the gain of dynodes number of dynodes by one and reduced the gain of dynodes and arrived at the 7 dynode PMT R12992-100, which showed a significantly improved pulse timing performance. As a by-product, on our request they re-arranged the dynode pins such as to provide the lowest possible pick-up noise from the envisaged Cockroft-Walton type custom-made high voltage (HV) power supply. Both the PMT types PMT R11920-100 and R12992-100 became commercial products, with the latter one as their final product for the CTA project.

ETE followed a path similar to Hamamatsu's one, at first developing demonstrator PMTs of optimized one selected parameter, as for example, the PMT type D872 as the QE demonstrator and the PMT type D569/2SA for low after-pulse and short pulse width. Later on they switched to the required 1.5' size, working on optimization of the requested set of parameters. ETE produced a 1.5' PMT D569/3SA of 8-dynodes, but later on because of our request of full-compatibility, switched to the 7-dynode version. The latest representative of this family that we tested has the label D573KFLSA. This PMT showed an even shorter pulse width and faster transit time spread compared to its predecessor with 8 dynodes. The probability of after-pulses is still high compared to the Hamamatsu PMTs and has to be significantly improved in the final product [6].

The tested PMTs from both companies show a peak quantum efficiency in the range 36-42%, along with high photo electron (ph.e.) collection efficiency (94.6% for 400 nm), short

pulse width and low after-pulse probability. On our request the newest ETE PMT has the same mechanical dimensions and output pins as the Hamamatsu R12992-100 and both PMTs can replace each other.

2.1 PMT Gain

Sensitivity to single photo-electrons (ph.e.) is a real advantage for precision measurements of light flux and for the evaluation of PMTs. For evaluating the single ph.e. sensitivity of test PMTs, we built a special low-noise setup which reduced the pick-up noise. The PMT under test was illuminated by a laser with a pulse width of about 50ps and a wavelength of 405nm. The laser light was fed into an graded-index optical fiber of 100m length. The purpose was to provide a time delay of 500ns for separating the light pulse from the pick-up noise of the laser power supply. The signal of the PMT was measured by a fast oscilloscope. We used a pulse generator for triggering the laser and the oscilloscope simultaneously. The PMT was inserted into a copper tube of ~ 25 cm length and 2mm wall thickness for shielding from electromagnetic pickup. We set the setup inside a Faraday cage professional room to further reduce pickup noise. We calculated the gain of the PMT from the charge produced by single ph.e.s. We decided that for the CTA project the PMTs will be operated at the gain of 40 k. For the selected custom-built amplifier we measured an equivalent noise of ~ 5000 electrons in 10ns time window. The chosen 40k gain provides a signal to noise ratio of ~ 8 , which provides a good shape for single ph.e. amplitude distribution. This low gain was selected for reducing the effect of *fatigue* (aging of dynode system) for PMTs because they will be operating in the presence of a strong, steady background emission from the Light of the Night Sky (LoNS). The chosen gain of 40k can be obtained when an average voltage of 880V is applied for the ETE PMTs and a slightly higher one, 960V for the Hamamatsu PMTs.

2.2. The ph.e. collection efficiency onto the first dynode

One of the main parameters of a light sensor is the photon detection efficiency (PDE). In the case of a PMT the PDE is the convolution of the QE with the ph.e. collection efficiency.

Both companies have undertaken a serious effort to optimize the ph.e. collection efficiency onto the first dynode. This is not a simple task because in the current design of PMTs only the electrostatic focusing is used for optimizing both the ph.e. collection efficiency and the short pulse width and Transit Time Spread (TTS). Optimization of one of the mentioned parameters can be done only at the expense of some degradation of the other parameter. So a reasonable compromise solution is needed for providing a good performance for a PMT. The parameter which can help optimizing both the ph.e. collection efficiency and the short pulse width is the electrostatic design of the input chamber of the PMT. By using three dimensional simulation codes for optimizing the tracks of ph.e. within the input chamber and by optimizing the radius of curvature of the input window both companies made a serious effort to maximize the ph.e. collection efficiency, keeping the pulse width below the requested 3ns. Hamamatsu reported a ph.e. collection efficiency of 94.6% for $\lambda=400$ nm and up to 98% for longer wavelengths for an applied voltage of 350V between the photo cathode and the first dynode.

The precise values from ETE PMT are not yet finalized, although these shall be similar to the results of Hamamatsu PMT.

So the reported record high ph.e. collection efficiency can be seen as equivalent to the increase in QE.

Unfortunately the so far known methods for measuring the ph.e. collection efficiency suffer from uncertainties and systematic errors in the order of 10% (or somewhat larger), so it is not straightforward to perform experimental comparison with simulation results.

2.3. Pulse Width

For measuring the pulse width, the PMT was illuminated with laser shots of ~ 10 ph.e intensity. The pulse shape was measured on a 4 GHz bandwidth oscilloscope. It was also measured as the FWHM of a Gaussian fit to the signal. Fig.1 shows the pulse width of a Hamamatsu 7-dynode PMT operated at a gain 40k. Hamamatsu PMTs show a pulse width of (3.0-3.2)ns at 40k gain. The 7 dynode ETE D573KFLSA PMTs show a pulse width of 2.5ns. This is an improvement of 0.5ns compared to the previous version from ETE with 8 dynodes.

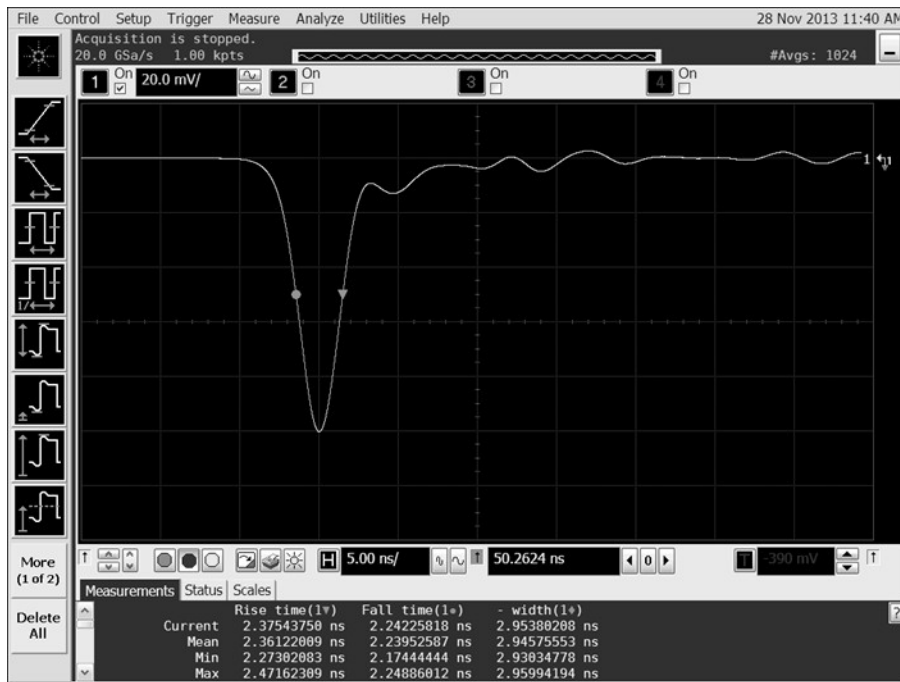


Fig.1. Pulse width of a Hamamatsu 7-dynode PMT measured on an oscillograph. The rise time is 2.4ns, fall time 2.2ns and the pulse width 3ns at a gain of 50k.

2.4. After-pulses

After-pulsing is a PMT-internal effect. One differentiates between light- and charge-induced after-pulsing. The latter is responsible for most of the unwanted rate. Triggered by the impinging photons, along with the genuine signal the PMT produces additional pulses, which are delayed in time. The main reason for after-pulsing is the ionization of the residual atoms and

molecules within the evacuated tube by the electrons that are kicked-out from the photo cathode and accelerated towards the first dynode. The produced positive ions are accelerated in the reverse direction towards the photo cathode and on impact release a relatively large number of

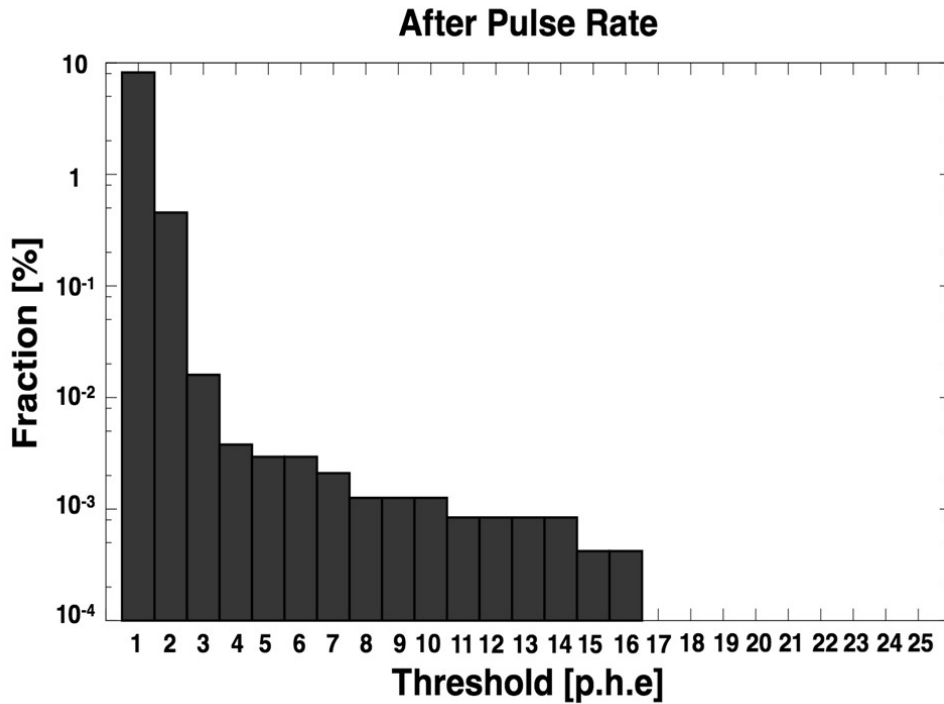


Fig.2. After-pulse rate of a 7-dynode Hamamatsu PMT, operated at a gain of 40k.

secondary electrons, which are accelerated towards the first dynode. Impurities in the form of different chemical elements and their compounds, which are adsorbed on the surface of the first dynode, play a dominant role for after-pulsing. The latter is a crucial parameter for PMTs especially when these are used in self-triggered mode. It defines the trigger threshold of an IACT [7]. Together with industrial partners we devoted quite some time and efforts for suppressing this negative effect. From our experience in evaluating PMT parameters for over 25 years, we learnt that on average a given PMT is producing an after-pulsing rate of $\sim 0.5\%$ (normalized to the genuine rate of signal ph.e.s), measured over the set threshold of 4ph.e. of a discriminator. The latter is the desired threshold value for operating individual PMTs in a multi-pixel imaging camera of an IACT. We requested from the manufacturers to reduce after-pulsing down to the level below 0.02%. Reducing the after-pulsing turned out to be quite a complex issue. In multiple design, production and test iterations the manufacturers significantly improved the level of evacuation of PMTs, see for example, Fig.2. They included a larger number of “getters” into the tube as well as critically reviewed and redesigned the space between the first dynode and the focusing metallic plate. The latter has a central hole through which the electrons are focused onto the first dynode.

2.4.1 Light-induced after-pulses

We measured after-pulses for a period from few tens of ns up to $5\mu\text{s}$ after the laser shot. During the measurement we set the high voltage to provide 40k gain and shot with a laser intensity of ~ 10 ph.e..

We noticed that quite some after-pulsing rate is due to the light emission of the dynode system. Details of these studies we reported in reference [8]. We measured the timing of light-induced after-pulses and images of PMTs, observing light glow from inter-dynode space. Also, we measured the spectrum of emitted light. It turned out that there is a sizable light emission not only from the surface of the dynodes, but also from the dynode holding mechanical structure. It turned out that the latter is a very good insulator and for example, in the case of Hamamatsu PMTs it is made from corundum with a small admixture of ruby. This structure has a strong light emission at $\sim 700\text{nm}$. Although at these wavelengths the alkali photo cathode of the tested PMTs has a very low sensitivity, nevertheless, because of the high intensity of light, the produced rate is quite intense. After we communicated our studies to the manufacturers they introduced some kind of baffles on the side of the dynode system, which reduced the chance for this secondary light emission finding a path back to the photo cathode.

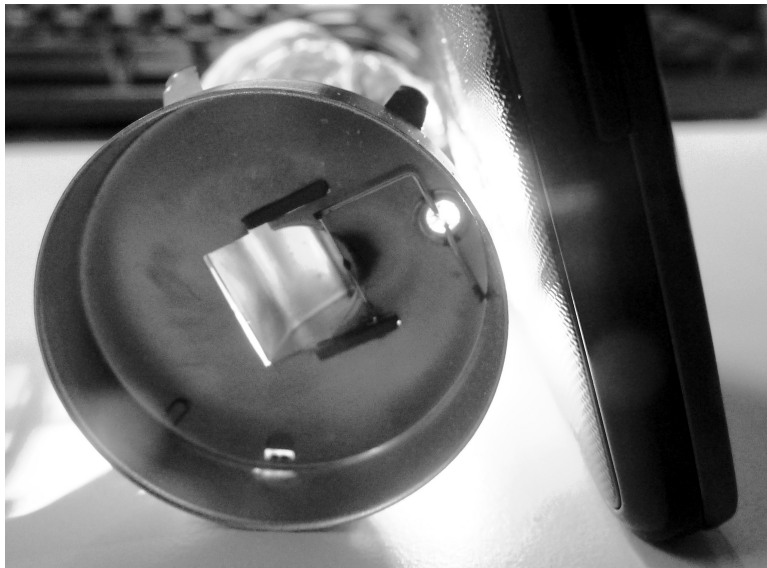


Fig.3. Head-on photo of a broken 7-dynode PMT Hamamatsu R12992-100. Through the square hole one can see the first dynode reflecting light. It is due to the illumination of the gaps between the dynodes 4-6 from the right side in the photo. Those dynodes guide the light back to the first dynode.

In Fig 3 we show the result of a simple test. We illuminated the dynodes 4-6 of a broken Hamamatsu PMT from one side and could observe some light coming out from the first dynode. This means that the dynodes of a PMT, despite their dark color and diffuse, absorbing surface, can work as a light guide (of a low efficiency), thus providing light-feedback to the photo cathode.

After all these studies we obtained PMTs with significantly reduced after-pulsing effect.

Fig.2 shows the dependence of the after-pulse probability on the threshold. The Hamamatsu PMTs fulfill the CTA requirement of 0.02% after-pulse probability at a set threshold of 4 ph.e.. During the earlier iteration cycles we obtained PMTs from ETE, which showed a very low after-pulsing level, conforming with the requirement of CTA. The few tested ETE PMTs from the latest iteration batch showed an after-pulse probability of 0.2%; these have to be improved by one order of magnitude. ETE explained to us that they are improving one parameter of a PMT at a time and in the latest batch the focus was on the fast timing. In the final product they plan to include all of the developed technologies for arriving at a really optimized PMT.

2.5. Anti-reflecting film between the entrance window glass and the photo cathode layer

One of the factors which contributed to the enhanced QE is due to the insertion of a thin anti-reflecting film between the PMT input glass window and the photo cathode material layer. Application of this film, typically of up to a few tens of nm thickness and of an intermediate refraction index n between that of the glass ($n \sim 1.5$) and the photo cathode ($n \sim 3$), can reduce the light reflected back from the PMT, so that more light will reach the photo cathode. The main task of inserting the thin film of selected material is solving the chemical compatibility and the long-term stability problems. According to data from developers in ETE (private communication) such a film can increase the average QE (wavelength dependent increase) by some 10-12 %.

2.6. Mat surface and convex shape for the input window

From our previous studies we learnt that a mat surface of the flat-shape input window can increase the QE by 6-8 %. The hemispherical-shape input mat window can increase the QE by up to 15 %; our earlier studies on this topic are reported in reference [9].

We requested the manufacturers to produce a slightly convex-shaped input window. This has two advantages: a) it has a better coupling with the light guides (in our case the non-imaging compound parabolic concentrators, the so-called Winston cones), providing an enhanced chance probability for the photons to interact with the photo cathode and as a result a higher QE and b) to provide better timing characteristics and photo-electron collection efficiency onto the first dynode.

Both manufacturers produced PMTs with convex-shape input window. Right from the beginning Hamamatsu used a novel technology for producing convex-shape mat input window for the 1.5' size PMTs. The PMTs from consecutive iteration cycles of ETE still have a clear input window, but they are planning to give the PMTs mat input window at a later stage.

2.7. Transit Time Spread

Transit time spread (TTS) is an effect caused by different distances between photo cathode and first dynode. Electrons from the center of the photo cathode have a shorter trajectory to the first dynode than those from the outer parts. This causes a time difference for

the arrival time of the signal. For the measurements we illuminate the whole photo cathode with the laser intensity inducing ~ 1 ph.e.. We measure a TTS of 2.4ns at 40 k gain for the Hamamatsu PMT R-12992-100. The latest ETE version D573KFLSA has a TTS of 1.4ns. ETE has reduced the TTS by 0.4ns switching from PMT D569/3SA (8 dynodes) to the 7 dynode version D573KFLSA.

2.8 HV distribution for providing the same gain for a large number of PMTs

From the previous experience we learnt that for providing the same gain for a large number of PMTs, as for example, in the imaging camera of an IACT, including several hundreds of PMTs, the applied HV differences can be as large as ~ 600 V (peak-to-peak). This is a real disadvantage because the transit time of the signal in different PMTs can differ on several nanoseconds. This makes the simple, fast coincidence trigger schemes inefficient or forces one to use individual delay lines, which unfortunately need to be re-adjusted with the aging of PMTs. For this reason we asked both companies if they could reduce this large spread in the applied HV for PMTs for obtaining the same gain. We understood that one of the reasons for the large spread was due to the temperature variation inside the factory where the PMTs are produced. One possibility could be trying to stabilize the temperature around the box where the different material evaporation and flow processes are taking place.

According to the available preliminary data we observed that the PMTs from Hamamatsu demonstrate HV distribution for obtaining the same gain that is about twice as narrow. Although this sounds as a novel and very attractive feature, it needs to be confirmed in future checks.

2.9. F-factor

By using a dedicated single ph.e. data analysis method developed by us some 15 years ago, we measured the noise factor F of the PMTs. We think it is not superfluous to mention here that the definition of the F -factor for a PMT, taken from the classical reference [10], is as follows:

$$F = [1 + \text{var}(q)/\langle q \rangle^2]^{0.5}$$

In the above formula $\text{var}(q)$ is the variation of the charge of the measured single ph.e. distribution, and $\langle q \rangle$ is its mean. The F -factor shows by how much the expected Poisson amplitude resolution of a PMT is degraded due to the dynode amplification system. Below we want to report in short the outline of the above mentioned method. At first we want to collect a possibly “pure” sample of single ph.e. events. For this we illuminate the PMT under test with pulses from a thermal source of light like, for example, a LED (this can be a reasonable assumption) and reduce the voltage applied to the LED until only $< 2\%$ of triggers produce single ph.e. charge in a PMT. This condition provides a negligibly small, below 1% contribution from 2ph.e. events in the single ph.e. distribution. Typically we measure the charge output of a PMT by using a FADC, either a stand-alone 2GSample/s, 700MHz bandwidth device from *Acqiris* or the one which is incorporated into a modern oscilloscope like from Tektronix of 4GHz bandwidth (a simple gated charge ADC like LeCroy 2249A is equally useful). Depending

on the gain of the test PMT it may become necessary to use some type of voltage (=current) amplifier with a fixed gain of 10-100. At first we measure the single ph.e. spectrum by applying $\sim 10^5 - 10^6$ triggers and collecting a single ph.e. distribution of $(2-20) \times 10^3$ events. Then we block the light path by using a remotely controlled beam interrupter (a piece of black paper will do the

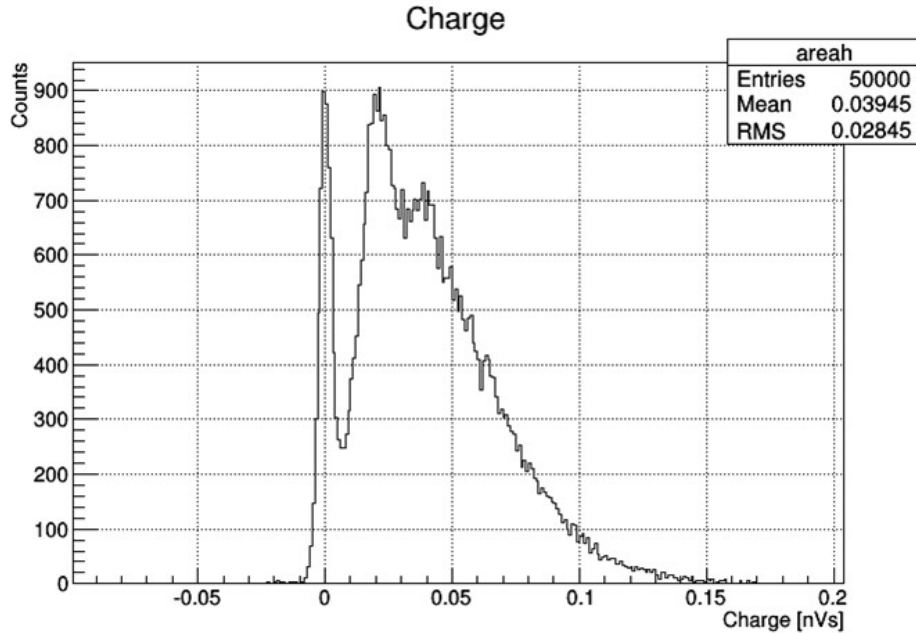


Fig.4. Single ph.e. resolution of a Hamamatsu R12992-100 PMT operated at a HV of 1300V. Along with the single ph.e. peak one can see also the second ph.e. peak.

job equally well) and collect a very comparable number of triggers (a pedestal file in fact). After this we select roughly the peak positions of both distributions and fit these with Gaussian function within ± 1 sigma range. From the fit we obtain the mean and the sigma of the distributions. If necessary we slightly shift the pedestal distribution along the x-axis for centering the peaks of both distributions to the same channel of FADC. Then we count the number of events below ± 1 sigma in both distributions and normalize the number of events in the pedestal file to the one in the distribution with signal. After this normalization we start subtracting, bin by bin, starting from the largest amplitudes in the signal distribution, the corresponding bin content of the pedestal distribution and check if the difference is above 5 sigma (the latter is defined as the square root from the sum of both bin contents). If the requested condition is fulfilled, we keep this signal. Coming closer and closer towards the center of the pedestal value, at some moment the difference starts to become less than the preset value. This is where we stop and obtain the final shape of the single ph.e. distribution. A somewhat higher precision may be achieved when loosening the check criteria from 5 sigma down to 4 sigma or even to 3 sigma. Such data treatment allows one to take into account the numerous genuine single ph.e. events of very small amplitudes which are masked by the few orders of magnitude more intense pedestal events. And it is well-known that hence these small amplitude ph.e. events are heavily contributing into the F -factor of a PMT.

The final PMT samples which we tested showed an outstanding amplitude resolution, see Fig.4 as an example. The measured peak/valley values were in excess of ≥ 3 . We measured F -factor values in the range of 1.06 – 1.08, which is very unusual; to the knowledge of authors never before such a good amplitude resolution has been reported for classical PMTs.

3. Conclusions

Both Hamamatsu and ETE in multiple iterations have developed and produced 1.5' size PMTs for the CTA project. These have a high quantum efficiency of 36-42 % and high ph.e. collection efficiency. Hamamatsu PMTs, meanwhile a commercial product, show a very low after-pulsing of $\leq 0.02\%$ for a set threshold of 4ph.e.. In the earlier production iteration cycles ETE also demonstrated a low after-pulse probability for test PMTs, but the few PMTs samples from their latest iteration showed a relatively high after-pulsing. While Hamamatsu PMTs show a pulse width of 3.2ns, the ETE PMTs show a pulse width of 2.5 ns and TTS 1.5 ns. ETE is going to finalize their PMT development program and produce PMTs where all the best features from their development work will be integrated. The main parameters of these PMTs are the best worldwide.

Acknowledgments

We acknowledge the CTA collaboration, the European FP7 program (FP7/2007–2013) under Grant agreement no. 262053, and the Max-Planck-Institute for Physics in Munich for supporting these products to become real and for allowing us evaluating some PMT samples.

References

- [1] B.S. Acharya et al., *Astroparticle Physics* 43 (2013) 318.
- [2] The H.E.S.S. project. (<http://www.mpi-hd.mpg.de/hfm/HESS/>).
- [3] The MAGIC project. (<http://magic.mpp.mpg.de/>).
- [4] The VERITAS project. (<http://veritas.sao.arizona.edu/>).
- [5] T. Toyama, et al., *Nucl. Instr. Meth. A* 787 (2015) 280.
- [6] R. Mirzoyan, et al., *Nucl. Instr. Meth. A*, [doi:10.1016/j.nima.2015.08.030](https://doi.org/10.1016/j.nima.2015.08.030)
- [7] R. Mirzoyan, et al., *Nucl. Instr. Meth. A* 387 (1997) 74.
- [8] M. Ahnen, et al., *IEEE Transact. Nucl. Sci.*, 62, No. 3, June 2015, 1313.
- [9] D. Paneque, et al., *Nucl. Instr. Meth. A* 518 (2004) 619.
- [10] A.G. Wright, *IEEE Transact. Nucl. Sci.*, NS 34, No 1, February 1987.